In Situ Monitoring of the Nascent *Pseudomonas fluorescens* Biofilm Response to Variations in the Dissolved Organic Carbon Level in Low-Nutrient Water by Attenuated Total Reflectance-Fourier Transform Infrared Spectroscopy[▽]

Anne Delille, Fabienne Quilès, and François Humbert*

*Laboratoire de Chimie Physique et Microbiologie pour l'Environnement, Nancy-Université, CNRS,
405, rue de Vandoeuvre, F-54600 Villers-lès-Nancy, France*

Drinking water quality management requires early warning tools which enable water supply companies to detect quickly and to forecast degradation of the microbial quality of drinking water during its transport throughout distribution systems. This study evaluated the feasibility of assessing, in real time, drinking water biostability by monitoring in situ the evolution of the attenuated total reflectance-Fourier transform infrared (ATR-FTIR) fingerprint of a nascent reference biofilm exposed to water being tested. For this purpose, the responses of nascent *Pseudomonas fluorescens* biofilms to variations in the dissolved organic carbon (DOC) level in tap water were monitored in situ and in real time by ATR-FTIR spectroscopy. Nascent *P. fluorescens* biofilms consisting of a monolayer of bacteria were formed on the germanium crystal of an ATR flowthrough cell by pumping bacterial suspensions in Luria-Bertani (LB) medium through the cell. Then they were exposed to a continuous flow of dechlorinated sterile tap water supplemented with appropriate amounts of sterile LB medium to obtain DOC concentrations ranging from 1.5 to 11.8 mg/liter. The time evolution of infrared bands related to proteins, polysaccharides, and nucleic acids clearly showed that changes in the DOC concentration resulted in changes in the nascent biofilm ATR-FTIR fingerprint within 2 h after exposure of the biofilm to the water being tested. The initial bacterial attachment, biofilm detachment, and regrowth kinetics determined from changes in the areas of bands associated with proteins and polysaccharides were directly dependent on the DOC level. Furthermore, they were consistent with bacterial adhesion or growth kinetic models and extracellular polymeric substance overproduction or starvation-dependent detachment mechanisms.

The biological stability of drinking water in distribution systems is a major concern of water supply companies (14), consumers, regulators, and public health authorities alike (1, 7). Bacterial regrowth within distribution systems is dependent upon a complex interaction of chemical, physical, operational, and engineering parameters (52). In particular, temperature, pH, disinfectant residual, hydrodynamic conditions, residence time, pipe materials, and above all the availability and composition of biodegradable organic matter are key factors in microorganism regrowth processes (37). Drinking water biostability is commonly assessed by biomass-based or biodegradability methods (37, 45, 47). Unfortunately, because of a slow response (usually more than 24 h) and/or batch processing these methods do not enable in situ real-time monitoring of microbiological quality. Moreover, culture-based methods do not reflect the actual dynamics of the attached bacterial films on pipe surfaces, which play a major role in postdisinfection biological regrowth (27, 33). Consequently, in addition to these methods, managing finished water quality requires early warning devices which enable workers to detect quickly, or even to forecast, degradation of drinking water quality. A possible strategy consists of monitoring continuously, in situ and in real time, the status of biofilm development on the inner surfaces of the distribution system by using electrochemical (6, 20, 22), optical (18, 19), or piezoelectric (34) sensors. Nevertheless, to date, most of these sensors have been developed solely on a laboratory scale.

During the past two decades, attenuated total reflectance-Fourier transform infrared (ATR-FTIR) spectroscopy has proven to be a useful analytical tool for monitoring biofilms in situ nondestructively in real time and under fully hydrated conditions (11, 19, 35). Furthermore, Boualam et al. (10) showed that biofilm monitoring by the ATR-FTIR technique is able to discriminate within 10 h water samples containing variable quantities of biodegradable organic matter. This result suggests that drinking water biostability could be assessed by monitoring the evolution of the ATR-FTIR spectrum of an appropriate reference biofilm exposed to the water being tested. This paper explores and develops this idea. For this purpose, the responses of nascent *Pseudomonas fluorescens* biofilms to variations in the dissolved organic carbon (DOC) in low-nutrient tap water were monitored by ATR-FTIR spectroscopy. *P. fluorescens* was chosen as the reference bacterium for several reasons: (i) it is present in drinking water distribution networks (46); (ii) it is able to grow in low-nutrient situations (50); (iii) it is used in a standard procedure used for measurement of assimilable organic carbon in water (4, 50); (iv) the *Pseudomonas* group is a good indicator of potential regrowth in water distribution systems (39); (v) and *P. fluorescens* has been widely used in model bacterial surface colonization studies (2, 15, 26, 36).

* Corresponding author. Mailing address: Laboratoire de Chimie Physique et Microbiologie pour l'Environnement, Nancy-Université, CNRS, 405, rue de Vandoeuvre, 54600 Villers-lès-Nancy, France. Phone: (33) 3 83 68 52 38. Fax: (33) 3 83 27 54 44. E-mail: francois .humbert@lcpme.cnrs-nancy.fr.
▽ Published ahead of print on 20 July 2007.

MATERIALS AND METHODS

Bacterial strain and culture conditions. The nonpathogenic strain *P. fluorescens* CIP 69.13 used in this study was obtained from the Pasteur Institute Collection (Paris, France). Stock cultures were maintained with the Microbank cryovial system (Pro-lab Diagnostics, Cheshire, United Kingdom) at −80°C. Bacteria were cultivated for 24 h at 27 ± 1°C in Luria-Bertani (LB) broth (25 g/liter; Difco Laboratories, Detroit, MI) with continuous stirring. Bacterial suspensions were then diluted 1:10 in fresh LB medium (25 g/liter) and incubated in 500-ml Erlenmeyer flasks at 27 ± 1°C. All solutions were prepared using deionized water (Milli-Q; Millipore Corp.).

Preparation of bacterial inocula. When the cells reached the end of the exponential growth phase, they were harvested by centrifugation ($10,000 \times g$, 10 min, 4°C), and the pellet was resuspended in sterile LB medium (0.5 g/liter). The bacterial concentration of the resulting suspension was adjusted to obtain an optical density at 620 nm of 0.28, equivalent to $\sim 10^8$ CFU/ml. The suspension was left at room temperature (21 ± 1°C) for 15 min on a magnetic stirrer before inoculation into the flow system.

Water samples. Water samples were taken from the drinking water distribution network of Villers-lès-Nancy (France) and were left uncovered for 24 h to dechlorinate them. They were then supplemented with different amounts of LB medium to obtain various DOC concentrations ranging from 1.5 to 11.8 mg/liter. All water samples were filter sterilized through 0.22-μm-pore-size membrane filters (Millipore Corp., Bedford, MA). The pH and ionic strength of solutions were 6.8 ± 0.1 and about 3 mM, respectively. The glassware used was heated at 550 ± 1°C for 4 h to remove any traces of carbon.

Bacterial enumeration procedures. Viable cell enumeration was done in triplicate on R2A agar (Merck, Darmstadt, Germany) by the spread plate technique. Counting was performed after incubation of plates at 21 ± 1°C for 48 h. The total cell number was determined by staining 1-ml portions of serial dilutions of the sample tested with 0.5 μl of SYBR green II (Molecular Probes, Eugene, OR) for 20 min in the dark. Then samples were vortexed for 1 min to disrupt any cell clumps, filtered through a 0.22-μm-pore-size Millipore polycarbonate membrane filter (Millipore Corp., Bedford, MA), and rinsed three times with nonpyrogenic sterile water (Aqua B; Braun, Melsungen, Germany). Membranes supporting bacteria were mounted on a glass microscope slide. Bacteria were counted using an Olympus BX51 epifluorescence microscope (Olympus Corp., Tokyo, Japan) equipped with a 100× (N.A. 1.30) oil immersion objective and an appropriate filter set (excitation wavelength, 488 nm; 500-nm long-pass dichroic mirror; 520- ± 10-nm band-pass emission filter). Images were collected using a Colorview III charge-coupled device camera from Soft Imaging System. All experiments were performed in triplicate.

DOC measurement. DOC concentrations were measured with a total organic carbon (TOC) analyzer (model 5050A; Shimadzu, Melbourne, Australia) according to standard method 5310B (4). Inorganic carbon was eliminated with phosphoric acid (Merck, Darmstadt, Germany) and by purified oxygen bubbling. Prior to each series of measurements, the TOC analyzer was calibrated with a potassium phthalate solution (Merck, Darmstadt, Germany). The detection limit was 0.1 mg/liter.

Flow system and ATR flow cell. The flow system used for growing biofilms and monitoring their evolution over time is shown in Fig. 1. It consisted of an inoculation flask that was placed onto the surface of a magnetic stirrer to provide constant mixing, an ATR-FTIR flow cell (SPECAC, Kent, United Kingdom), a peristaltic pump (Minipuls 3; Gilson's, Villiers-le-Bel, France), and a waste reservoir, all connected by silicone tubing (inside diameter, 5 mm; Versilic). The ATR-FTIR flow cell was designed to enclose a trapezoidal crystal (72 by 10 by 6 mm) with an incidence angle of 45°, yielding six internal reflections on the upper face in contact with the sample. The ATR cell was sealed with Kalrez O-rings. Prior to each experiment, the flow cell was dismantled, cleaned with a 2% (vol/vol) Triton X-100 solution, and successively rinsed with hot tap water, ethanol, hot tap water again, and finally nonpyrogenic sterile water. Immediately after this cleaning process, the flow cell was reassembled and connected to the flow system by sterile silicone tubing. The whole flow system was then disinfected with 70% ethanol for 5 h and rinsed with nonpyrogenic sterile water for 24 h. The cleaning and disinfection procedure quality was controlled both by ATR-FTIR spectroscopy and by counting bacterial cells in water samples taken at the inlet and outlet of the flow system.

ATR-FTIR analysis. (i) Spectral acquisition. ATR-FTIR spectra were recorded between 4,000 and 800 cm^{-1} with a Vector 22 spectrometer (Bruker, Karlsruhe, Germany) equipped with a KBr beam splitter and a deuterated triglycine sulfate thermal detector. The resolution of the single-beam spectra was 4 cm^{-1}. The number of bidirectional double-sided interferogram scans was 100, which corresponded to a 1-min accumulation. All interferograms were Fourier
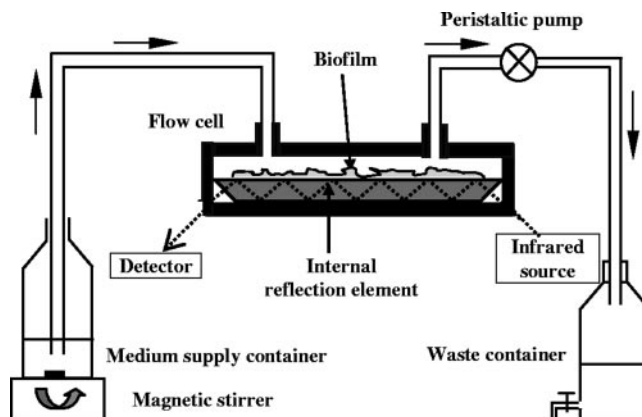

FIG. 1. Schematic diagram of the experimental setup used for growing *P. fluorescens* biofilms on the ATR crystal surface and monitoring changes in the biofilm ATR-FTIR fingerprint in real time.

processed using the Mertz phase correction mode and a Blackman-Harris three-term apodization function. FTIR measurements were performed at 21 ± 1°C in an air-conditioned room and in the dark. The following appropriate spectra were used to remove the spectral background: an LB medium reference spectrum for the bacterial pellet spectrum and, for biofilm monitoring experiments, a sample reference spectrum acquired immediately before the step being studied. Water vapor subtraction and baseline correction were performed when necessary. Recording of spectra, data storage, and all manipulations were performed using the OPUS 3.1 software (Bruker, Karlsruhe, Germany). In the course of biofilm monitoring experiments, ATR-FTIR spectra were recorded every 10 or 30 min.

(ii) Sampling depth. In ATR-FTIR spectroscopy, the sample (the rare medium) is placed in contact with the ATR crystal (the dense medium), an internal reflection element (IRE) with a high refractive index (Fig. 1). The infrared beam is focused onto the edge of the IRE, multiply reflected on the inner surface of the ATR crystal, and then directed to a suitable detector. At each reflection at the sample-ATR crystal interface, an evanescent wave is created in the rare medium, where it can be absorbed. The electric field amplitude of this evanescent wave decays exponentially with distance from the crystal surface. The penetration depth (d_p) of the evanescent wave is defined as the distance at which the evanescent wave drops to e^{-1} times its intensity at the surface of the IRE. It is determined by the following equation: $d_p = \lambda/[2\pi (n_c^2 \sin^2\theta - n_s^2)^{1/2}]$, where λ is the wavelength of the incident radiation, n_c is the refractive index of the IRE, n_s is the refractive index of the rare medium in contact with the IRE, and θ is the angle of incidence (21). For all experiments, a germanium IRE with a θ of 45° and an n_c of 4.0 was used. Considering the anomalous dispersion of water and the refraction index of bacterial components in the mid-infrared region (5, 38), the n_s of the rare medium was estimated to be around 1.43 ± 0.1. Thus, the depths of penetration were calculated to be 0.22 ± 0.01, 0.42 ± 0.01, and 0.59 ± 0.01 μm at 2,990, 1,550, and 1,100 cm^{-1}, respectively. Consequently, only bacteria that were immediately adjacent to the crystal surface were detected. The IRE surface area exposed to cell suspensions was approximately 8 by 48 mm.

Biofilm development on the IRE surface. Inoculation and introduction of a water sample into the flow system were carried out under sterile conditions, carefully avoiding formation of air bubbles in the flow cell. The flow rate was maintained at 0.7 ml/min.

(i) Initial attachment of bacteria. After cleaning and disinfection procedures, the flow cell was successively and aseptically supplied with (i) sterile LB medium (0.5 g/liter) for 24 h to establish a conditioning film on the IRE surface and to provide a background spectrum for the subsequent bacterial spectra and (ii) a bacterial suspension containing $\sim 10^8$ CFU/ml in sterile LB medium (0.5 g/liter) for 3 h to initiate attachment of *P. fluorescens* bacteria to the IRE. The inflow tubing of the ATR cell was then replaced by new sterile silicone tubing to avoid bacterial contamination of the subsequent water samples.

(ii) Influence of DOC level on the evolution of nascent *P. fluorescens* biofilms. Nascent biofilms were exposed to sterile LB medium (0.5 g/liter, corresponding to 165 mg DOC/liter) for 3 h to promote *P. fluorescens* biofilm development and/or to a series of dechlorinated and sterile water samples containing DOC at concentrations ranging from 1.5 to 11.8 mg/liter. Samples were pumped through the ATR cell at a rate of 0.7 ml/min for 15 to 50 h. When the solution was
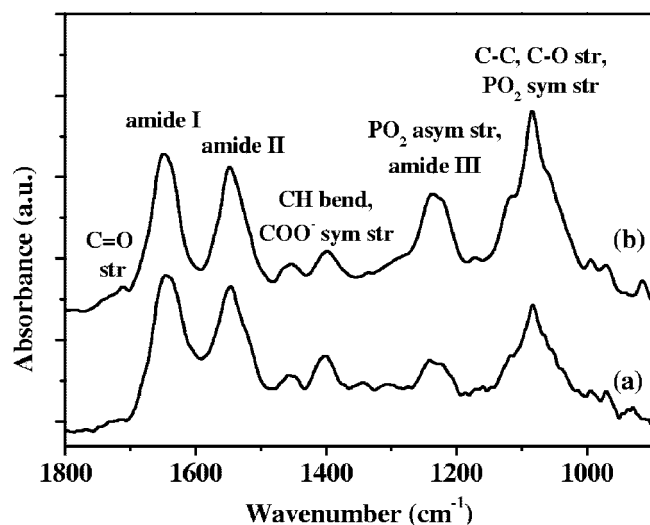
FIG. 2. ATR-FTIR spectra of *P. fluorescens* planktonic bacteria harvested at the end of the exponential phase (spectrum a) and a 6-h-old *P. fluorescens* biofilm formed by successive flow of a bacterial suspension for 3 h and sterile LB medium (0.5 g/liter) over the germanium IRE (spectrum b). The spectra have been vertically shifted for clarity and normalized to the amide II band. str., stretch; sym., symmetric; asym., asymmetric; a.u., arbitrary units.
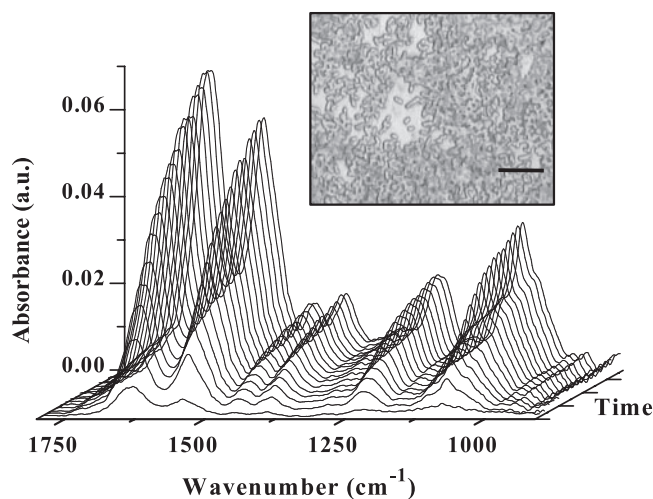

FIG. 3. Temporal evolution of ATR-FTIR spectra during initial attachment of *P. fluorescens* to the germanium IRE. A suspension containing bacteria at the end of the exponential phase ($\sim 10^8$ CFU/ml) in sterile LB medium (0.5 g/liter) was introduced into the flow cell at time zero and flowed through the cell for 3 h. The optical microscope image (magnification, ×100) shows the nascent *P. fluorescens* biofilm attached to the Ge IRE after the 3-h inoculation period. Bar = 10 µm. a.u., arbitrary units.

changed, an air bubble was passed through the flow system under sterile conditions so that solutions did not mix as far as possible.

RESULTS AND DISCUSSION

ATR-FTIR fingerprint of planktonic and biofilm *P. fluorescens*. Figure 2 compares representative ATR-FTIR spectra of a pellet of planktonic *P. fluorescens* bacteria at the end of the exponential phase and a 6-h *P. fluorescens* biofilm formed on the germanium IRE. These spectra are typical of bacteria and have been assigned previously (17, 19). They exhibit major bands at around 3,400 cm^{-1} (O—H stretch), 3,300 cm^{-1} (N—H stretch), 2,900 cm^{-1} (C—H stretch) (data not shown), 1,648 cm^{-1} (amide I; mainly C=O stretch), 1,548 cm^{-1} (amide II; N—H bend and C—N stretch), 1,456 cm^{-1} (C—H bend), 1,400 cm^{-1} (partially due to a symmetric stretch of the carboxylate ions), 1,235 cm^{-1} (P=O asymmetric stretch, C—O—C stretch, and amide III [C—N bend and N—H stretch]), and the 1,150- to 900-cm^{-1} region, referred to below as the PS band (P=O symmetric stretch, C—C and C—O stretch). The main groups of biomolecules which can be associated with these bands are proteins (amide I, II, and III bands), nucleic acids (regions around 1,240 and 1,080 cm^{-1}), polysaccharides (region from 1,150 to 900 cm^{-1}), and lipids (region around 2,900 cm^{-1}). Interestingly, the band relative intensities in the two spectra were different, and in particular, the amide II/PS band intensity ratio was higher in the 6-h biofilm spectrum and this ratio varied with the age and the physiological state of biofilm, as discussed further below.

Initial attachment of *P. fluorescens* to the germanium ATR crystal. To initiate formation of a biofilm on the IRE, the flow cell was inoculated for 3 h with a suspension containing bacteria at the end of the exponential phase ($\sim 10^8$ CFU/ml) in sterile LB medium (0.5 g/liter). This 3-h period proved to be relevant for forming nascent biofilms which resulted in ATR-FTIR spectra that had good signal-to-noise ratios but were far from saturation. The latter point was essential to detect under good conditions all subsequent spectral changes of a nascent biofilm in response to environmental parameter changes. ATR-FTIR spectra acquired over this period (Fig. 3) were similar to planktonic bacterium spectra (Fig. 2), in particular, regarding the relative intensities and the amide II/PS band intensity ratio. As illustrated in Fig. 4 for the amide II band, the intensity of all bands increased with time. These results reflected accumulation of biomass on the IRE surface and an increase in the IRE surface coverage by bacteria. Optical microscope images of 3-h biofilms showed *P. fluorescens* cells arranged mainly as a monolayer on the IRE surface (Fig. 3). The surface coverage of bacteria was 65% ± 15%. These results are in agreement with a previous study of Korber et al. (26) which reported that *P. fluorescens* bacteria obeyed monolayer attachment kinetics and the saturation of surfaces by a monolayer of colonizing bacteria does not equal the total available area during attachment of *P. fluorescens*. As observed previously in similar experiments with *Pseudomonas aeruginosa* (25), the rate of increase was reduced as the surface coverage increased. For this attachment period, the plot of the amide II band area (*A*) versus time can be fitted using the following equation: $A = A_{max}(1 - e^{-kt})$, where A_{max} is the amide II band area corresponding to a complete bacteria single layer, *k* is an absorption rate constant, and *t* is time (Fig. 4a). It should be noted that small changes in the culture conditions, growth phase, or number of bacteria inoculated into the flow system may slightly modify adhesion kinetics (54) and/or result in the appearance of a latency period before colonization (44). However, we observed that the differences in adhesion kinetics did not alter the subsequent response of the nascent biofilms to environmental condition changes.
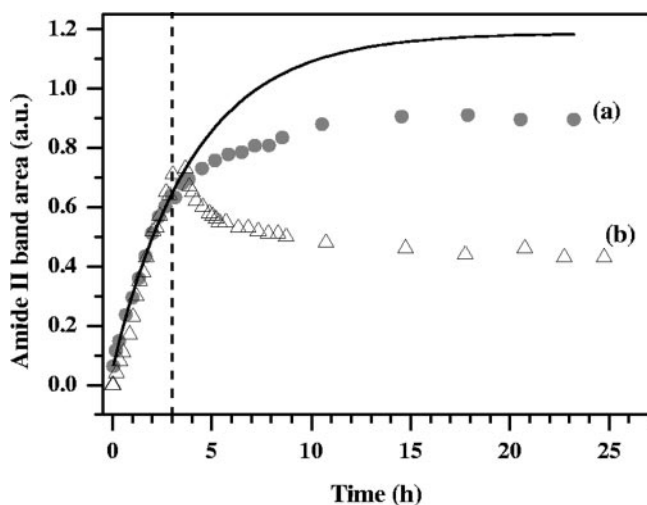
FIG. 4. Impact of the drastic reduction in the DOC level on development of nascent *P. fluorescens* biofilms attached to the Ge crystal. After 3 h of inoculation (dashed line), nascent biofilms were exposed to LB medium (165 mg DOC/liter) (experiment a) and dechlorinated sterile tap water (2.8 mg DOC/liter) (experiment b) under flow conditions. The solid line represents the nonlinear regression fit determined only for the data set for the 3-h inoculation period of experiment a using the equation $A = A_{max}(1 - e^{-kt})$ ($k = 0.24$ h^{-1}; regression coefficient $R^2 = 0.997$). a.u., arbitrary units.

Nascent biofilm development under LB medium flow conditions. After 3 h of inoculation, only sterile LB medium was pumped through the system, with the pH and ionic strength constant. Although bacteria were no longer supplied, the intensity of all bands continued to increase, as shown in Fig. 4a for the amide II band. This increase reflected biofilm development and bacterial cells dividing on and colonizing the IRE surface (11) and producing extracellular polymeric substances (EPS) (16, 29). The overproduction of EPS by bacterial cells during attachment to an inert substratum is well documented (3, 12, 13, 41, 51). As previously reported (9, 16), the polysaccharide band increased at a higher rate than the amide I and amide II bands and the bands in the 1,240-cm^{-1} region. After LB medium flowed for about 15 h, the area of all bands reached a plateau. Unlike the findings of Bremer and Geesey (11), no sudden increase in the absorbance was observed when the bacterial inoculum was replaced with a sterile LB medium flow. This indicates that the absorbance increase over the 3-h inoculation period was due not only to bacterial deposition on the IRE surface but also partially to bacterial growth and EPS secretion. At the end of the inoculation period, the latter two mechanisms widely prevailed over deposition. Furthermore, it should be noted that passage of an air bubble through the flow cell between the bacterial and LB medium flows did not result in changes in the ATR-FTIR spectra, demonstrating that, unlike the findings of Suci et al. (43), the nascent biofilm was not altered significantly and the distance of attached bacteria from the IRE surface remained unchanged.

Nascent biofilm development under dechlorinated sterile drinking water flow conditions. As shown in Fig. 4b for the amide II band, development of a 3-h biofilm was quite different in tap water that was much less nutritive than 0.5-g/liter LB medium containing 165 mg DOC/liter, when all other param-

eters, including the temperature, pH, ionic strength, flow rate, and oxygen concentration, were identical in the two experiments. The intensity of all bands stopped increasing and declined rapidly within 1 h after the bacterial suspension was replaced with dechlorinated sterile drinking water containing 2.8 mg DOC/liter. Whereas steady absorbance was observed within 1 min after the pH or ionic strength was changed (30), the absorbance decreased continuously for about 20 h and then plateaued. This result is consistent with the suggestion that nascent biofilms of *P. fluorescens* partially detached in response to nutrient stress, as reported previously by Delaquis et al. (15). Allison et al. (2) suggested that the enzymatic degradation of EPS has a specific role in the detachment of *P. fluorescens* biofilms under starvation conditions. Moreover, as reported previously (23, 53), cells grown in rich nutrient-containing LB medium are more sensitive to transfer to low-nutrient medium.

Nascent biofilm response to variations in DOC level in tap water over a 12-day period. To confirm the previous findings and to explore the evolution of the nascent *P. fluorescens* biofilm response to variations in the DOC level over the course of time, a 3-h *P. fluorescens* biofilm was successively subjected to sterile LB medium and a series of sterile drinking water samples with DOC levels ranging from 1.5 to 11.8 mg/liter for durations of exposure between 15 and 50 h. As shown by the evolution of the amide II band area in Fig. 5, any variation in DOC level rapidly modified the kinetics of biofilm development. The response time was 1 to 2 h. For water samples containing DOC at a concentration less than about 5.3 mg/liter, the intensity of all bands continuously decreased in the first 15 to 20 h, reflecting, as shown previously (Fig. 4b), gradual detachment induced by starvation. Conversely, for water samples containing more than 5.3 mg DOC/liter, the intensity of all bands increased again, indicating that there was biofilm regrowth on the IRE surface. This biofilm regrowth is highlighted in Fig. 6 in the case of the water sample containing 11.8 mg DOC/liter. Over the course of this stage the amide II/PS band intensity ratio changed little and was similar to the ratio observed during the initial attachment period, suggesting that biofilm regrowth was mainly due to the growth of surface-attached bacteria. As shown in Fig. 6, the amide II band area increased exponentially with time, indicating that there was exponential lateral growth of bacteria still attached to the surface at this time. Assuming that the increase in the amide II band area was approximately proportional to the increase in the number of bacteria on the surface, the fit displayed in Fig. 6 yielded a specific growth rate of 0.36 h^{-1}, which was higher than the specific planktonic growth rate of 0.23 h^{-1} determined in suspension cultures. A shorter generation time in biofilms than in planktonic populations has been observed previously during early biofilm formation (8). Furthermore, this growth rate in biofilms is consistent with the growth rates reported by Mueller (32) for *P. aeruginosa* and *P. fluorescens* biofilms on stainless steel. As clearly shown in Fig. 5, detachment and regrowth rates were dependent on the DOC level. In addition, the biofilm response was quite reproducible over the course of the experiment, and similar DOC levels resulted in qualitatively similar responses. However, it was difficult to establish an acute relationship between detachment and regrowth rates and the DOC level. This could have been due to
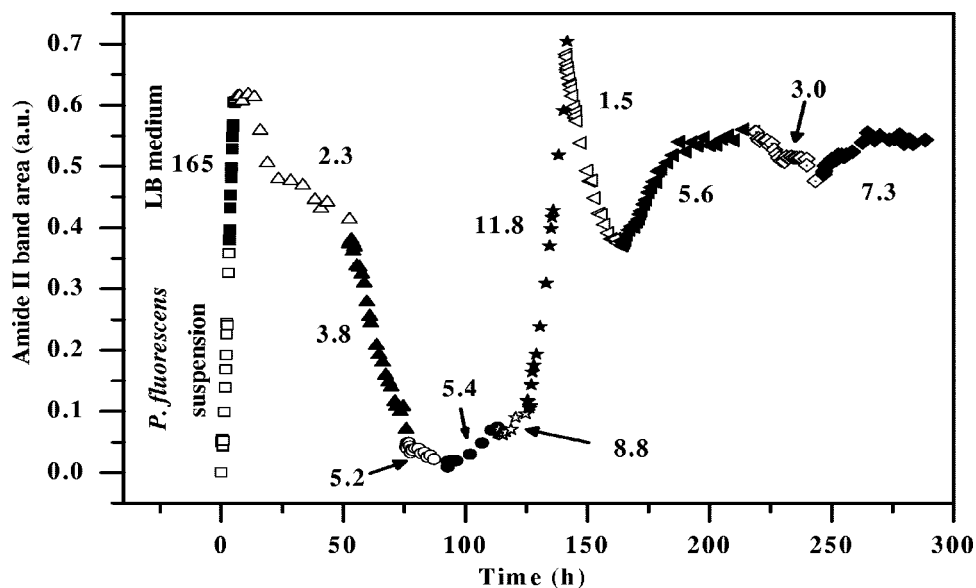
FIG. 5. Effect of DOC level changes on *P. fluorescens* biofilm development monitored by changes in the amide II band area. After the 3-h inoculation period (□), the nascent biofilm attached to the Ge IRE was subjected to sterile LB medium for 3 h (■) and then a series of dechlorinated sterile drinking water samples containing various DOC levels under flow conditions. The DOC level (in mg/liter) is indicated for each water sample. a.u., arbitrary units.

ageing of the reference biofilm and, in particular, changes in the physiological state of bacteria over the course of the experiment. Indeed, the physiological state of bacteria which regrew after starvation should have been different from that of the original bacteria which grew in the nutrient-rich LB medium. Previous studies demonstrated that a range of different bacteria display enhanced adhesion after starvation or after growth in low-nutrient medium (24) and that bacterial cells grown under low-nutrient conditions are physiologically more tolerant than bacterial cells isolated from higher-nutrient con-

FIG. 6. Exponential fit of the amide II band area change with time when the nascent *P. fluorescens* biofilm was exposed to dechorinated drinking water containing 11.8 mg DOC/liter, the eighth stage in Fig. 5. The time origin corresponds to the moment when the water sample was introduced into the flow cell. (regression coefficient $R^2 = 0.996$). a.u., arbitrary units.

ditions (23, 53). This also could explain why the response amplitude appeared to decrease over time and the spectral profile changed after 125 h, particularly in the PS region (data not shown).

Figure 5 might suggest that an in-line TOC or DOC analyzer could allow us to assess drinking water biostability. In fact, a number of studies have shown (40, 49) that TOC and DOC are inadequate for this purpose because the ratio of biodegradable or assimilable organic matter to TOC or DOC is highly variable. This is why the standard methods for assessing the biostability of drinking water rely upon the determination of biodegradable DOC and assimilable organic carbon (47). However, these methods also have limitations. They are batch methods which require several-day assays. Moreover, depending on the treatment, the standard organic carbon biodegradability measurements (assimilable organic carbon, biodegradable DOC, and DOC) can give contradictory results for the biostability of a given water sample (42). Indeed, many factors other than organic carbon can promote or limit microbial growth (28, 31, 47). In contrast, the method presented here does not have these limitations because it monitors directly and in situ the development of a nascent reference biofilm exposed to the water being tested. Unlike the biofilm formation rate method (48), no sampling is required. Therefore, any factor promoting significant regrowth or detachment of the nascent reference biofilm can be detected even if this factor is below the detection limits of conventional analytical techniques. Nonetheless, it is noteworthy that in this first feasibility study of such a biosensor, deterioration of drinking water microbiology quality was promoted by adding a few milligrams of LB broth per liter. LB complex broth provides numerous nutrients (amino acids, nucleic acids, a variety of trace carbohydrates, etc.) which can also be provided by most organic matter present in drinking water. The advantages of using LB broth in
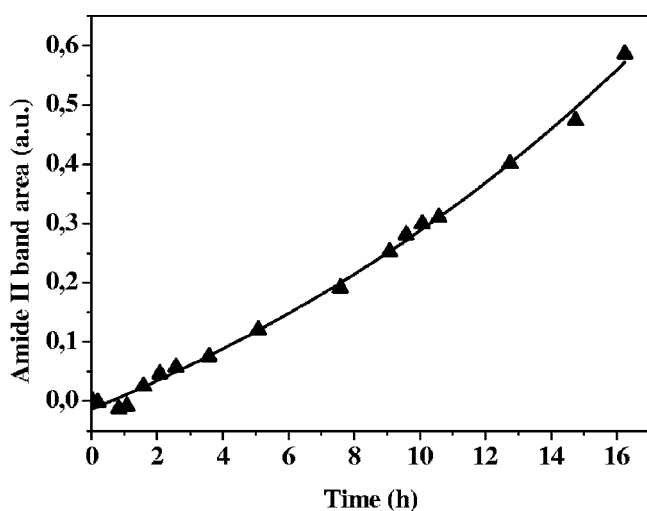
this first study as a biodegradable organic matter supplement were that the amount of the supplemented assimilable organic matter was controlled and there was a large panel of nutrients. Yet, further investigations are now needed to determine to what extent the reported findings depend on the nature of the organic matter present in drinking water.

In conclusion, the results presented in this paper support the idea that in situ and in real time, drinking water biostability can be monitored via a biosensor based on the ATR-FTIR fingerprint of a nascent reference biofilm through a bypass system in order to avoid any contamination of the water being tested. In comparison with the established methods for assessing drinking water biostability, the major advantages of using such a biosensor should be (i) an early warning capacity (within 2 h), in particular because the reference biofilm is nascent, (ii) in situ assessment of drinking water biostability, and (iii) sensitive detection of any factor promoting biofilm growth, not only changes in the organic carbon concentration. However, further investigations are needed to confirm and extend the results of the present study and to consider implementation of such a biosensor in real drinking water systems. In particular, studies are currently being carried out in three main areas: (i) enhancement of biosensor sensitivity by optimizing reference biofilm formation, (ii) improvement of the correlation between nascent biofilm detachment or growth rate and the nature of the biodegradable organic matter, and (iii) evaluation of the effect of other parameters, such pH, temperature, disinfectant concentration, and hydrodynamic conditions, on the nascent reference biofilm response.

ACKNOWLEDGMENTS

REFERENCES

1. **Allan, I. J., B. Vrana, R. Greenwood, G. A. Mills, B. Roig, and C. Gonzalez.** 2006. A "toolbox" for biological and chemical monitoring requirements for the European Union's Water Framework Directive. Talanta **69:**302–322.
2. **Allison, D. G., B. Ruiz, C. Sanjose, A. Jaspe, and P. Gilbert.** 1998. Extracellular products as mediators of the formation and detachment of Pseudomonas fluorescens biofilms. FEMS Microbiol. Lett. **167:**179–184.
3. **Allison, D. G., and I. W. Sutherland.** 1987. The role of exopolysaccharides in adhesion of freshwater bacteria. J. Gen. Microbiol. **133:**1319–1327.
4. **American Public Health Association, American Water Works Association, and Water Environment Association.** 1998. Standard methods for the examination of water and wastewater. American Public Health Association, American Water Works Association, and Water Environment Association, Washington, DC.
5. **Arakawa, E., T. P. S. Tuminello, B. N. Khare, and M. E. Milham.** 1997. Optical properties of horseradish peroxidase from 0.13 to 2.5 μm. Biospectroscopy **3:**73–80.
6. **Auret, L., and J. Desmarest.** 2005. Un concept innovant en matière de qualité de l'eau: le capteur de détection biofilm. Eau Ind. Nuis. **283:**61–63.
7. **Bartram, J., J. Cotruvo, M. Exner, C. Fricker, and A. Glasmacher (ed.).** 2003. Heterotrophic plate counts in drinking-water safety. IWA Publishing, London, United Kingdom.
8. **Bester, E., G. Wolfaardt, L. Joubert, K. Garny, and S. Saftic.** 2005. Planktonic-cell yield of a pseudomonad biofilm. Appl. Environ. Microbiol. **71:**7792–7798.
9. **Bosch, A., D. Serra, C. Pietro, J. Schmitt, D. Naumann, and O. Yantorno.** 2006. Characterization of Bordetella pertussis growing as biofilm by chemical analysis and FT-IR spectroscopy. Appl. Microbiol. Biotechnol. **71:**736–747.
10. **Boualam, M., F. Quilès, L. Mathieu, and J. C. Block.** 2002. Monitoring the effect of organic matter on biofilm growth in low nutritive waters by ATR/FT-IR spectroscopy. Biofouling **18:**73–81.
11. **Bremer, P. J., and G. G. Geesey.** 1991. An evaluation of biofilm development utilizing non-destructive attenuated total reflectance Fourier transform infrared spectroscopy. Biofouling **3:**89–100.
12. **Cheung, H. Y., S. Q. Sun, B. Sreedhar, W. M. Ching, and P. A. Tanner.** 2000. Alterations in extracellular substances during the biofilm development of Pseudomonas aeruginosa on aluminum plates. J. Appl. Microbiol. **89:**100–106.
13. **Costerton, J. W.** 1985. The role of bacterial exopolysaccharides in nature and disease. Dev. Ind. Microbiol. **26:**249–261.
14. **Delahaye, E., Y. Levi, G. Leblon, and A. Montiel.** 2006. A simple system for biofilm potential monitoring in drinking water. J. Basic Microbiol. **46:**22–27.
15. **Delaquis, P. J., D. E. Caldwell, J. R. Lawrence, and A. R. McCurdy.** 1989. Detachment of Pseudomonas fluorescens from biofilms on glass surfaces in response to nutrient stress. Microb. Ecol. **18:**199–210.
16. **Donlan, R. M., J. A. Piede, C. D. Heyes, L. Sanii, R. Murga, P. Edmonds, I. El-Sayed, and M. A. El-Sayed.** 2004. Model system for growing and quantifying Streptococcus pneumoniae biofilms in situ and in real time. Appl. Environ. Microbiol. **70:**4980–4988.
17. **Filip, Z., and S. Hermann.** 2001. An attempt to differentiate Pseudomonas spp. and other soil bacteria by FT-IR spectroscopy. Eur. J. Soil Biol. **37:**137–143.
18. **Flemming, H. C., and A. Tamachkiarow.** 2003. Monitoring of biofilms in technical systems—a crucial component of advanced anti-fouling strategies. Water Sci. Technol. Water Supply **3:**199–204.
19. **Geesey, G. G., and P. A. Suci.** 2000. Monitoring biofilms by Fourier transform infrared spectroscopy, p. 253–277. In L. V. Evans (ed.), Biofilms: recent advances in their study and control. Harwood Academic Publishers, Amsterdam, The Netherlands.
20. **Gião, M. S., M. I. Montenegro, and M. J. Vieira.** 2003. Monitoring biofilm formation by using cyclic voltammetry—effect of the experimental conditions on biofilm removal and activity. Water Sci. Technol. **47:**51–56.
21. **Harrick, N. J.** 1985. Internal reflexion spectroscopy. Harrick Scientific Corporation, Ossining, NY.
22. **Herbert-Guillou, D., B. Tribollet, D. Festy, and L. Kiéné.** 1999. In situ detection and characterization of biofilm in waters by electrochemical methods. Electrochim. Acta **45:**1067–1075.
23. **Horowitz, A., M. I. Krichevsky, and R. M. Atlas.** 1983. Characteristics and diversity of subarctic marine oligotrophic, stenoheterotrophic, and euryheterotrophic bacterial populations. Can. J. Microbiol. **29:**527–535.
24. **James, G. A., D. R. Korber, D. E. Caldwell, and J. W. Costerton.** 1995. Digital image analysis of growth and starvation responses of a surface-colonizing Acinetobacter sp. J. Bacteriol. **177:**907–915.
25. **Kang, S. Y., P. J. Bremer, K. W. Kim, and A. J. McQuillan.** 2006. Monitoring metal ion binding in single-layer Pseudomonas aeruginosa biofilms using ATR-IR spectroscopy. Langmuir **22:**286–291.
26. **Korber, D. R., J. R. Lawrence, and D. E. Caldwell.** 1994. Effect of motility on surface colonization and reproductive success of Pseudomonas fluorescens in dual-dilution continuous culture and batch culture systems. Appl. Environ. Microbiol. **60:**1421–1429.
27. **Lechevallier, M. W., W. Schultz, and R. G. Lee.** 1991. Bacterial nutrients in drinking water. Appl. Environ. Microbiol. **57:**857–862.
28. **Lehtola, M. J., I. T. Miettinen, T. Vartiainen, and P. J. Martikainen.** 2002. Changes in content of microbially available phosphorus, assimilable organic carbon and microbial growth potential during drinking water treatment processes. Water Res. **36:**3681–3690.
29. **Marcotte, L., G. Kegelaer, C. Sandt, J. Barbeau, and M. Lafleur.** 2007. An alternative infrared spectroscopy assay for the quantification of polysaccharides in bacterial samples. Anal. Biochem. **361:**7–14.
30. **McWhirter, M. J., P. J. Bremer, and A. J. McQuillan.** 2002. Direct infrared spectroscopic evidence of pH- and ionic strength-induced changes in distance of attached Pseudomonas aeruginosa from ZnSe surfaces. Langmuir **18:**1904–1907.
31. **Miettinen, I. T., T. Vartiainen, and P. J. Martikainen.** 1997. Phosphorus and bacterial growth in drinking water. Appl. Environ. Microbiol. **63:**3242–3245.
32. **Mueller, R. F.** 1996. Bacterial transport and colonization in low nutrient environments. Water Res. **30:**2681–2690.
33. **Ndiongue, S., P. M. Huck, and R. M. Slawson.** 2005. Effects of temperature and biodegradable organic matter on control of biofilms by free chlorine in a model drinking water distribution system. Water Res. **39:**953–964.
34. **Nivens, D. E., J. Q. Chambers, T. R. Anderson, and D. C. White.** 1993. Long-term, on-line monitoring of microbial biofilms using a quartz crystal microbalance. Anal. Chem. **65:**85–89.
35. **Nivens, D. E., J. Schmit, J. Sniatecki, T. Anderson, J. Q. Chambers, and D. C. White.** 1993. Multichannel ATR/FT-IR spectrometer for on-line examination of microbial biofilms. Appl. Spectrosc. **47:**668–671.
36. **O'Toole, G. A., and R. Kolter.** 1998. Initiation of biofilm formation in Pseudomonas fluorescens WCS365 proceeds via multiple, convergent signalling pathways: a genetic analysis. Mol. Microbiol. **28:**449–461.
37. **Prévost, M., P. Laurent, P. Servais, and J. C. Joret (ed.).** 2005. Biodegrad-

able organic matter in drinking water treatment and distribution. AWWA, Denver, CO.

38. **Reiter, G., M. Siam, D. Kalkenhagen, W. Gollneritsch, D. Baurecht, and U. P. Fringeli.** 2002. Interaction of a bacterial endotoxin with different surfaces investigated by in situ Fourier transform infrared attenuated total reflection spectroscopy. Langmuir **18:**5761–5771.

39. **Ribas, F., J. Perramon, A. Terradillos, J. Frias, and F. Lucena.** 2000. The Pseudomonas group as an indicator of potential regrowth in water distribution systems. J. Appl. Microbiol. **88:**704–710.

40. **Rizet, M., F. Fiessinger, and N. Houel.** 1982. Bacterial regrowth in a distribution system and its relationship with the quality of the feed water: case studies, p. 1199–1214. *In* Proceedings of the AWWA Water Quality Technology Conference, Miami Beach. AWWA, Denver, CO.

41. **Sauer, K., and A. K. Camper.** 2001. Characterization of phenotypic changes in *Pseudomonas putida* in response to surface-associated growth. J. Bacteriol. **183:**6579–6589.

42. **Sharp, R. R., A. K. Camper, J. J. Crippen, O. D. Schneider, and S. Leggiero.** 2001. Evaluation of drinking water biostability using biofilm methods. J. Environ. Eng. **127:**403–410.

43. **Suci, P. A., K. J. Siedlecki, R. J. J. Palmer, D. C. White, and G. G. Geesey.** 1997. Combined light microscopy and attenuated total reflection Fourier transform infrared spectroscopy for integration of biofilm structure, distribution, and chemistry at solid-liquid interfaces. Appl. Environ. Microbiol. **63:**4600–4603.

44. **Suci, P. A., J. D. Vrany, and M. W. Mittelman.** 1998. Investigation of interactions between antimicrobial agents and bacterial biofilms using attenuated total reflection Fourier transform infrared spectroscopy. Biomaterials **19:**327–339.

45. **Toze, S.** 1999. PCR and the detection of microbial pathogens in water and wastewater. Water Res. **33:**3545–3556.

46. **Van der Kooij, D.** 1977. The occurrence of *Pseudomonas* spp. in surface water and in tap water as determined on citrate media. Antonie Leeuwenhoek **43:**187–197.

47. **Van der Kooij, D.** 2003. Managing regrowth in drinking-water distribution systems, p. 199–232. *In* J. Bartram, J. Cortuvo, M. Exner, C. Fricker, and A. Glasmacher (ed.), Heterotrophic plate counts and drinking-water safety. IWA Publishing, London, United Kingdom.

48. **Van der Kooij, D., H. R. Veenendaal, C. Baars-Lorist, D. W. van der Klift, and Y. C. Drost.** 1995. Biofilm formation on surfaces of glass and Teflon exposed to treated water. Water Res. **29:**1655–1662.

49. **Van der Kooij, D., A. Visser, and W. A. M. Hijnen.** 1982. Determining the concentration of easily assimilable organic carbon in drinking water. J. Am. Water Works Assoc. **74:**540–545.

50. **Van der Kooij, D., A. Visser, and J. P. Oranje.** 1982. Multiplication of fluorescent pseudomonads at low substrate concentrations in tap water. Antonie Leeuwenhoek **48:**229–243.

51. **Vandevivere, P., and D. L. Kirchman.** 1993. Attachment stimulates exopolysaccharide synthesis by a bacterium. Appl. Environ. Microbiol. **59:**3280–3286.

52. **Volk, C. J., and M. W. Lechevallier.** 1999. Impacts of the reduction of nutrient levels on bacterial water quality in distribution systems. Appl. Environ. Microbiol. **65:**4957–4966.

53. **Walker, S. L.** 2005. The role of nutrient presence on the adhesion kinetics of *Burkholderia cepacia* G4g and ENV435g. Colloids Surf. B Biointerfaces **45:**181–188.

54. **Walker, S. L., J. E. Hill, J. A. Redman, and M. Elimelech.** 2005. Influence of growth phase on adhesion kinetics of *Escherichia coli* D21g. Appl. Environ. Microbiol. **71:**3093–3099.